Nonlinear-optical loop mirror demultiplexer using a random birefringence fiber: comparisons between simulations and experiments

Mark F. Arend, Michael L. Dennis, and Irl N. Duling III

Code 5671, Naval Research Laboratory, Washington, D.C. 20375-5338

Ekaterina A. Golovchenko, Alexei N. Pilipetskii, and Curtis R. Menyuk

Department of Computer Science and Electrical Engineering, University of Maryland Baltimore County, Baltimore, Maryland 21228-5398

Received March 17, 1997

A numerical simulation of the switching characteristics of a polarization multiplexed nonlinear-optical loop mirror demultiplexer is presented and compared with experiment. The model assumes that the optical fiber that composes the loop has a randomly varying birefringence, that the signal and the control pulses have the same frequency, and that these pulses are nearly solitons. Factors that affect the shape and the width of the switching window curve are discussed. A phase-dependent modulation of the switching window curve, which is due to incomplete averaging of the light polarization state, is observed both experimentally and numerically. Models in which the randomness is neglected are not able to describe this modulation adequately. © 1997 Optical Society of America

Demultiplexing data channels that are transmitted at 100-Gbit/s rates requires the design and development of advanced all-optical devices. The possible use of a nonlinear-optical loop mirror (NOLM) as the demultiplexing element in high-data-rate communication systems has been reported by a number of authors.[1] One forms the NOLM by joining each of the two ends of an optical fiber to a four-port fiber coupler to make a Sagnac interferometer. Switching is accomplished by introduction of a relative phase shift between the two counterpropagating signal pulses through cross-phase modulation induced by a control pulse. A relative timing jitter between the control pulse and the signal pulse often occurs in practice, and the demultiplexer must allow for this by having a switching window that is significantly broader than the individual pulses. Recently a numerical study of a NOLM demultiplexer showed that a broader switching window can be obtained by incorporation of soliton dragging effects if the fiber that composes the loop has low birefringence and the background random birefringence is negligible.[2]

In this Letter we report computer simulations of a NOLM demultiplexer for which the birefringence of the loop fiber is assumed to vary randomly, as is the case for standard communication fiber. Polarization mode dispersion in these types of fiber is a major obstacle in high-bit-rate systems. Our model takes into account the effect of a polarization controller and clarifies some effects that are apparent on the length scales over which our device operates and that cannot be explained with simpler models. The simulations are compared with experimental results that were reported previously,[3] showing excellent agreement.

A schematic illustration of the demultiplexer is shown in Fig. 1. The pulse stream to be demultiplexed enters the device at the signal-in port. A 50/50 coupler and a fiber loop constitute the Sagnac interferometer. Polarization multiplexing allows the control pulse to copropagate with the clockwise propagating portion of the signal pulse (the control pulse energy and the copropagating signal pulse energy are equal, and their carrier frequencies are the same). In the absence of a control pulse the device acts as a mirror, and the signal returns to the input. When the control pulse is present, the copropagating signal pulse experiences an additional phase shift, $\Delta\phi$, that is due to cross-phase modulation relative to the counterclockwise propagating signal pulse. At the coupler, the pulses interfere and produce an output at the signal-out port. Random variations in the birefringence axis of the fiber alter the polarization state of the light propagating around the loop. Therefore it is necessary to insert a polarization-controlling device, such as a linear retarder, into the loop to ensure that there is no control leakage out the signal-out port.

The coupled nonlinear Schrödinger equations that describe propagation in a birefringent fiber in normalized units are[4]

$$\begin{aligned} i\left(\frac{\partial u}{\partial \xi} + \delta\,\frac{\partial u}{\partial s}\right) + \frac{\beta}{2}\,u + \frac{1}{2}\,\frac{\partial^2 u}{\partial s^2} + i\,\frac{\alpha}{2}\,u \\ = -\left(|u|^2 + \frac{2}{3}\,|v|^2\right)u - \frac{1}{3}\,v^2 u^*, \\ i\left(\frac{\partial v}{\partial \xi} - \delta\,\frac{\partial v}{\partial s}\right) - \frac{\beta}{2}\,v + \frac{1}{2}\,\frac{\partial^2 v}{\partial s^2} + i\,\frac{\alpha}{2}\,v \\ = -\left(|v|^2 + \frac{2}{3}\,|u|^2\right)v - \frac{1}{3}\,u^2 v^*, \end{aligned} \tag{1}$$

where u and v are the normalized complex field envelopes along the slow and fast polarization axes in the fiber, respectively, ξ and s are normalized distance

0146-9592/97/120886-03$10.00/0

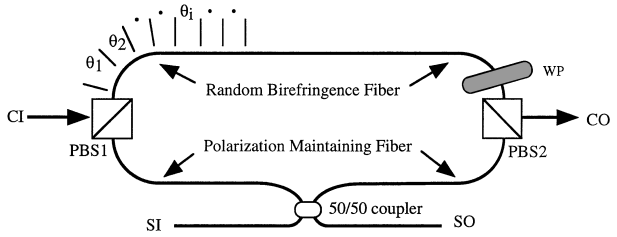

Fig. 1. (a) Schematic illustration of the demultiplexer: PBS1, PBS2, polarization beam splitters; SI, signal-in port; SO, signal-out port; CI, control-in port; CO, control-out port; WP, wave plate (or polarization controller).

and retarded time, respectively, β is the wave-number difference between the two principal polarizations at the same central frequency ($2\pi/\beta$ is the normalized beat length), $2\delta = \partial\beta/\partial\omega$ is the inverse group-velocity difference, and α is the normalized attenuation coefficient. It is natural to normalize the field amplitudes with respect to the soliton power P_0 and the time to the pulse's FWHM t_0, in which case the length must be normalized to $z_d = (t_0/1.76)^2\,(2\pi c/D\lambda^2)$, which is both the dispersive and the nonlinear length scale for a fundamental soliton, where D is the dispersion, λ is the wavelength, and c is the speed of light.

In a fiber with randomly varying birefringence, the polarization state of a pulse varies randomly with distance, so when the propagation length is long, the nonlinear terms and the group-velocity dispersion terms average over all the polarization states on the Poincaré sphere. The pulse propagation in that case can be described by use of the Manakov equation.[5] However, our goal is to develop a model of a nonlinear loop mirror that does not limit us to long fiber lengths, and therefore the full set of Eqs. (1) is used.

The equations are solved numerically by a split-step Fourier method.[6] Randomly varying birefringence is modeled by random rotation of the fiber birefringence axis by an amount $\Delta\theta = (\pi/4)\,(3l_s/z_h)^{1/2}\,\mathrm{ran}(-1,1)$ at the beginning of each propagation step of size l_s, where $\mathrm{ran}(-1,1)$ is a uniform random function on the interval $(-1,1)$. The parameter z_h is known as the decorrelation length.[7] This definition for $\Delta\theta$ corresponds to a random walk of the birefringence angle equal to $\pi/2$ in a distance z_h. For these studies we took z_h to be 30 m. The value for $l_s \ll l_c$ was chosen to be small enough that numerical errors were insignificant and was typically 0.2 m or less.

We implement the polarization controller numerically by multiplying the field by the appropriate Jones matrix $\mathbf{J}$ for a linear retarder of orientation γ and retardance ψ, where $J_{11} = \cos(\psi/2) - i\sin(\psi/2)\cos(2\gamma)$, $J_{12} = -i\sin(\psi/2)\sin(2\gamma)$, $J_{21} = J_{12}$, and $J_{22} = J_{11}{}^*$.[8] We found values for γ and ψ by allowing the control pulse to propagate around the loop in the absence of the signal pulse. By requiring that the resultant field, with components u_c and v_c, be transformed by the retarder so that its $\hat{u}$ component is extinguished and defining the phase difference $\varphi = \arctan[\mathrm{Im}(u_c)/\mathrm{Re}(u_c)] - \arctan[\mathrm{Im}(v_c)/\mathrm{Re}(v_c)]$, then

$$\gamma = \frac{1}{2}\arctan\left(\frac{-|u_c|}{|v_c|\cos\varphi}\right),$$

$$\psi = 2\arctan\left(\frac{-|u_c|}{|v_c|\sin\varphi\,\sin(2\gamma)}\right). \qquad (2)$$

The field that propagates in the counterclockwise direction must pass through the linear retarder in the opposite direction before propagating around the loop, so the appropriate Jones matrix by which to multiply this field is nearly the same as $\mathbf{J}$, with J_{12} becoming $-J_{12}$ and J_{21} becoming $-J_{21}$.

To simulate the experiment accurately[3] it was necessary to characterize the fiber in the loop mirror. A fiber of length $L = 1$ km was wound on a 16-cm-diameter spool. Given that the cladding diameter was 125 mm, we can conclude that the stress-induced linear birefringence was less than 10^{-7}, and circular birefringence could be ignored.[9] A nominal birefringence of the order of $\Delta n = 2 \times 10^{-7}$ and a polarization mode dispersion $\Delta\tau < 100$ fs were estimated experimentally by the frequency domain technique.[10] The dispersion parameter D was 5.45 ps/nm/km, and the physical attenuation coefficient α/z_d was measured to be 0.13 km^{-1}.

As the experimental source generated transform-limited pulses, we determined the input pulse width used for the simulations by fitting the experimental spectrum to a sech^2 spectrum. The experimental pulse width of $t_0 = 1.54$ ps was used in the simulations. By comparing the experimental and theoretical spectra of the switched pulse, we obtained a good estimate of the pulse energy. Figure 2(a) shows both the experimental spectrum and the one obtained from a simulation assuming that the signal pulse energy at the input port, W_0, was 1.36 times the energy of a soliton.

We calculated the switching characteristics by keeping only the final clockwise propagating component u_{cw} and the final counterclockwise propagating component u_{ccw}, which are passed by the polarizing beam splitters. For a given delay between the input control and signal pulses, we calculated the fractional transmitted energy by integrating the quantity $T = |u_{\mathrm{cw}} - u_{\mathrm{ccw}}|^2/W_0$. Figure 2(b) shows a plot of T as a function of delay, along with the related experimental trace. Near zero delay, where $\Delta\phi \geq \pi$, the switching window is somewhat insensitive to changes in $\Delta\phi$, and in fact a certain amount of overswitching was observed. Even though this effect flattens the top of the switching window (makes it more square) and is the reason for the dip in the curve very close to zero delay where $\Delta\phi > \pi$, it may be detrimental to the operation of the demultiplexer, depending on the threshold level required for switching. It should be noted that the vertical scale in Fig. 2(b) is not a free parameter, inasmuch as W_0 was found from the fit in Fig. 2(a) and all the parameters involved in producing this fit were determined experimentally.

The simulation shown in Fig. 2(b) assumes that the phase difference between control and signal pulses, $\Delta\Phi$, is zero independently of time delay. However, the high-frequency fluctuations shown in the experimental

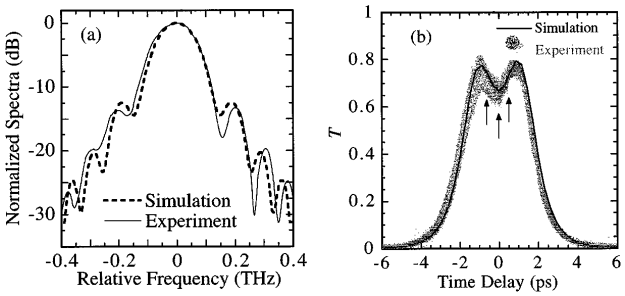

Fig. 2. (a) Plot of the power spectrum of the signal switched out of the demultiplexer. Sidebands are generated by the interference between the dispersive wave and the soliton component. (b) Plot of the experimental and the simulated switching windows, i.e., the transmitted power, T, as a function of time delay between control pulse and signal pulse. The simulation assumes a fixed phase difference between control and signal pulses. The arrows indicate the location of the plots in Fig. 3.

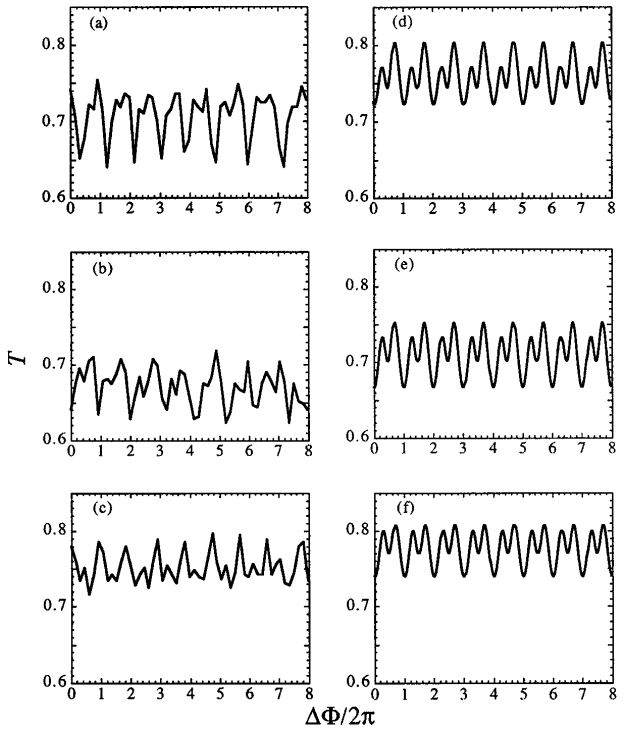

Fig. 3. Detailed view of Fig. 2(b). (a), (b), (c) Experimental traces at time delays of −0.6, 0, and 0.5 ps, respectively. (d), (e), (f) The corresponding responding simulations. The x axis has been converted into a phase delay for these plots.

trace of Fig. 2(b) are a consequence of the time-delay dependence of $\Delta\Phi$. Figure 3 shows a more detailed view of the experimental trace at the three time delays marked by the arrows in Fig. 2(b). The x axis is represented as a phase delay in Fig. 3. The simulations corresponding to the experimental traces are also shown in Fig. 3. Each of these simulations assumes a fixed time delay but a variable phase. By trying different random sequences we found that the exact shape of the curves in Fig. 3 depends on the precise configuration of the random birefringence. However, we found that there is reasonable qualitative agreement between experiment and simulation in that the amplitudes of the modulations are approximately the same. The amplitude of the modulation does not vary significantly as z_h is varied by an order of magnitude. However, the modulation tends to zero as z_h tends to zero. We compared the simulations shown in Fig. 3 with the results from a model based on the Manakov equations and found that it is not possible to explain the interference effects with the Manakov model because the loop length is small compared with the length scale over which the polarization state of the light uniformly samples the Poincaré sphere (~4 km according to our simulations).

In summary, we have investigated the switching characteristics of a NOLM demultiplexer, using a model that assumes that the fiber's axes of birefringence are randomly varying, as is the case in standard communication fiber, and that takes into account the effect of a polarization controller. This model allows us to explain effects that are important to the successful operation of a loop mirror demultiplexer that cannot be explained with models in which the randomization of the birefringence is ignored or averaged.

We acknowledge useful discussions with T. F. Carruthers and W. K. Burns. The research at the University of Maryland Baltimore County was supported by the National Science Foundation, the U.S. Department of Energy, and the Advanced Research Projects Agency through the U.S. Air Force Office of Scientific Research. Research at the Naval Research Laboratory (NRL) was supported by the Office of the Chief of Naval Research. This study was performed while M. Arend held a National Research Council–NRL Research Associateship.

References

1. K. Uchiyama, H. Takara, S. Kawanishi, T. Morioka, and M. Saruwatari, Electron. Lett. **28,** 1864 (1992); J. D. Moores, K. Bergman, H. A. Haus, and E. P. Ippen, Opt. Lett. **16,** 138 (1991); N. A. Whitaker, Jr., H. Avromopoulos, P. M. W. French, M. C. Gabriel, R. E. Lamarche, D. J. Giovanni, and H. M. Presby, Opt. Lett. **16,** 1838 (1991).
2. G. R. Williams, M. Vaziri, K. H. Ahn, B. C. Barnett, M. N. Islam, K. O. Hill, and B. Malo, Opt. Lett. **20,** 1671 (1995).
3. M. L. Dennis, M. F. Arend, and I. N. Dulling III, Photon. Technol. Lett. **8,** 906 (1996).
4. C. R. Menyuk, IEEE J. Quantum Electron. **QE-23,** 174 (1987); G. Agrawal, *Nonlinear Fiber Optics* (Academic, San Diego, Calif., 1995), Chap. 7.
5. S. G. Evangelides, L. F. Mollenauer, J. P. Gordon, and N. S. Bergano, J. Lightwave Technol. **10,** 28 (1992); P. K. A. Wai, C. R. Menyuk, and H. H. Chen, Opt. Lett. **16,** 1231 (1991).
6. C. R. Menyuk, J. Opt. Soc. Am. B **5,** 392 (1988).
7. C. R. Menyuk and P. K. Wai, J. Opt. Soc. Am. B **11,** 1288 (1994).
8. R. M. A. Azzam and N. M. Bashara, *Elipsometry and Polarized Light* (North-Holland, Amsterdam, 1977).
9. S. C. Rashleigh, J. Lightwave Technol. **1,** 312 (1983).
10. C. D. Poole and D. L. Favin, J. Lightwave Technol. **12,** 917 (1994).